Proceedings of the 19th International Symposium on the
Packaging and Transportation of Radioactive Materials
PATRAM 2019
August 4-9, 2019, New Orleans, LA, USA

Measurement of the Thermal Accommodation Coefficient between Helium and a Stainless Steel Surface

Cody Zampella, Mitchell Lane, Mustafa Hadj Nacer and Miles Greiner
Department of Mechanical Engineering, University of Nevada, Reno, NV, USA

Abstract

The vacuum drying process is commonly used to remove moister from used nuclear fuel casks before they are transferred to long-term storage facilities. During this process, the pressure in the cask may be reduced to as low as 67 Pa (0.5 Torr) to promote evaporation and removal of moisture. The low-pressure conditions during vacuum drying may cause the cladding temperature to considerably increase due to the effect of gas rarefaction. At these low pressures, a temperature-jump develops at the gas-solid interfaces and acts as a thermal resistance to heat transfer. This temperature-jump is characterized by the thermal accommodation coefficient.

The objective of this work is to design and acquire data from a concentric cylinders experiment that will be used to benchmark computational fluid dynamics simulations of rarefied gas heat transfer during vacuum drying. The experiment consists of two long concentric cylinders spaced by a 2-mm gap. The inner cylinder consists of a heater rod inserted into a thick aluminum cylinder covered with a thin stainless steel sheath. The outer cylinder consists of a pressure vessel whose temperature is controlled using a water chiller. The thermal accommodation coefficient is determined by measuring the difference in temperature between the inner and outer cylinder using thermocouples and comparing the results to an analytical expression in the slip and continuum regimes.

Introduction

Used nuclear fuel (UNF) assemblies spend several years in a cooling water pool before being transferred into a dry storage cask. The cask transfer operation takes place underwater, where a lift takes UNF assemblies from the slots in the pool and places them into the cask. After filling the cask with fuel assemblies, a lid is either bolted or welded to the cask. Once sealed, the cask is lifted out of the cooling pool and the water inside is drained by forcing helium through the vent port at the cask lid and withdraws water through a tube that reaches close to the cask bottom. The draining process leaves behind some water in the internal surfaces, which may cause corrosion of the internal structures or formation of a flammable mixture of oxygen and hydrogen by radiolysis [1]. To avoid these issues, the remaining water must be removed by a process such as vacuum drying.

Vacuum drying involves reducing the internal pressure of the cask below the vaporization pressure of water, promoting evaporation. This process is done in cycles of reducing the pressure and maintaining it at different levels to avoid the formation of ice in the vacuum lines [2]. A cask is considered to be dry when its internal pressure is maintained under 3 Torr (~400Pa) over 30 minutes after disconnecting the vacuum pump [3].

After the dryness criteria is achieved, an inert gas such as helium or nitrogen is pumped into the cask to increase the pressure up to 7atm. Containment is achieved by sealing the cask, making it ready for transfer to a storage pad on site, or transport off-site.

During vacuum drying, the internal pressure of the cask can be reduced to as low as 67 Pa [3]. At these low pressures, buoyancy-induced fluid motion and natural convection are minimal, leaving only radiation and conduction as heat transfer mechanisms to remove heat from the fuel assemblies. Another consequence of the low-pressure conditions is the gas rarefaction, which causes the temperature of the fuel rods to increase due to the temperature-jump at the gas-solid interfaces [4]. This temperature jump increases as the pressure decreases and acts as a thermal resistance to conduction heat transfer.

Federal regulation (10CFR72) [5] requires that "The spent fuel cladding must be protected during storage against the degradation that leads to gross ruptures or the fuel must be otherwise confined such that the degradation of the fuel during storage will not pose operational safety problems with respect to its removal from storage." It is important that the integrity of the cladding material is not compromised, even after decades in storage. Nuclear fuel assemblies must be transportable in case new regulations are created for reprocessing or disposal. A major factor for the loss of cladding integrity is the formation of radial hydrides, which leads to embrittlement [5].

Radial hydride formation happens when the cladding material reaches or exceeds a temperature of about 400°C (673K) in any operation (drying, transfer, transport, or storage), as specified by the Nuclear Regulatory Commission (NRC) Interim Staff Guidance-11, Revision 3 (ISG-11)[6]. This guidance was created to avoid the dissolution of circumferential hydrides that exist in the cladding. High temperatures also increase the internal pressure, leading to high hoop stresses within the cladding [7]. This causes the cladding material to become brittle if radial hydrides form, making them more vulnerable during an accident scenario [8, 9]. Vacuum drying is the most likely event to cause the cladding temperature to exceed 400°C [10] due to the effect of gas rarefaction.

The long term objective of this work is to experimentally benchmark computational fluid dynamics (CFD) models of heat transfer at low pressures that can be used to accurately predict the temperature of UNF casks during vacuum drying. The objective of this paper is to experimentally measure heat transfer through a 2-mm gap between two concentric cylinders filled with rarefied helium, and determine the thermal accommodation coefficient of helium on a stainless steel surface. The thermal accommodation coefficient is used to characterize the temperature jump at low pressures.

Gas Rarefaction

As the pressure decreases in a system, the number of collisions between molecules decreases. This leads to fewer collisions between molecules and between molecules and walls. A reduced number of collisions cause less heat transfer and discontinuity of macroscopic properties such as velocity, temperature, and partial pressure at the gas-solid interfaces. As pressure decreases, the level of gas rarefaction increases.

To determine the level of rarefaction of gas, the Knudsen Number, Kn,

$$Kn = \frac{\lambda}{L_C}, \tag{1}$$

defined as the ratio of the mean free path, λ, to the characteristic length of a system, L_C, is often employed. The characteristic length is typically the smallest length within the system.

The mean free path is defined as the average distance traveled by gas molecules between successive collisions [11] and is expressed as

$$\lambda = \frac{\mu}{P}\sqrt{\frac{2k_B T}{m}}, \tag{2}$$

where μ is the dynamic viscosity, P is the pressure, k_B is the Boltzmann constant (k_B = 1.38 ×10^{-23} J/K), T is the temperature, and m is the mass of the gas molecule.

The temperature dependent dynamic viscosity is determined as

$$\mu = \mu_0 \left(\frac{T}{T_0}\right)^{\frac{1}{2}}, \tag{3}$$

where T_0, is the reference temperature and μ_0 is the reference viscosity at the reference temperature (μ_0 =1.86×10^{-5} Pa.s at T_0 = 273.15 K) [12].

Using the Knudsen number, four regimes of rarefaction can be characterized as follows [4]:

- Continuum Regime ($Kn \leq 10^{-3}$), where the Navier-Stokes and Convective Energy equations may be used with no-slip boundary conditions.
- Slip Regime ($10^{-3} \leq Kn \leq 10^{-1}$), where the Navier-Stokes and Convective Energy equations still apply for gas far from the wall but slip boundary conditions of velocity, temperature and partial pressure should be employed at the gas-solid interface.
- Transitional Regime ($10^{-1} \leq Kn \leq 10$), where the collisional Boltzmann equation must be used. The Navier-Stokes equation, even with slip boundary condition, is no longer capable of solving the flow and heat transfer in this regime.
- Free Molecular Regime ($Kn > 10$), where the collisionless Boltzmann equation can be used to solve for flow and heat transfer.

It should be reminded here that this classification is not strict. The limits between the regimes shown have to be taken as an order of magnitude because the transition between regimes is not brutal but progressive.

Based on the internal pressure and characteristic length of UNF casks, vacuum drying occurs in the slip regime. At this regime of rarefaction, the Navier-Stokes equation subjected to the temperature jump boundary conditions can be used to model heat transfer. This temperature jump acts as a resistance to heat conduction [13]. Therefore, the temperature inside the cask is higher at low pressures compared to normal or atmospheric pressure [4].

The temperature jump boundary condition at the gas-solid interfaces can be expressed as [13]

$$T_g - T_w = \zeta_t \lambda \left.\frac{\partial T}{\partial y}\right|_w, \tag{4}$$

where T_g is the gas temperature, T_w is the wall temperature, ζ_T is the temperature jump coefficient, and y is the coordinate normal to the wall.

Several models for temperature jump coefficient have been proposed in the literature. Using the Lin and Willis model [14], the temperature jump coefficient can be written as

$$\zeta_T = \frac{\sqrt{\pi}\gamma}{(\gamma+1)\mathrm{Pr}}\left(\frac{2-\alpha}{\alpha} + 0.17\right), \tag{5}$$

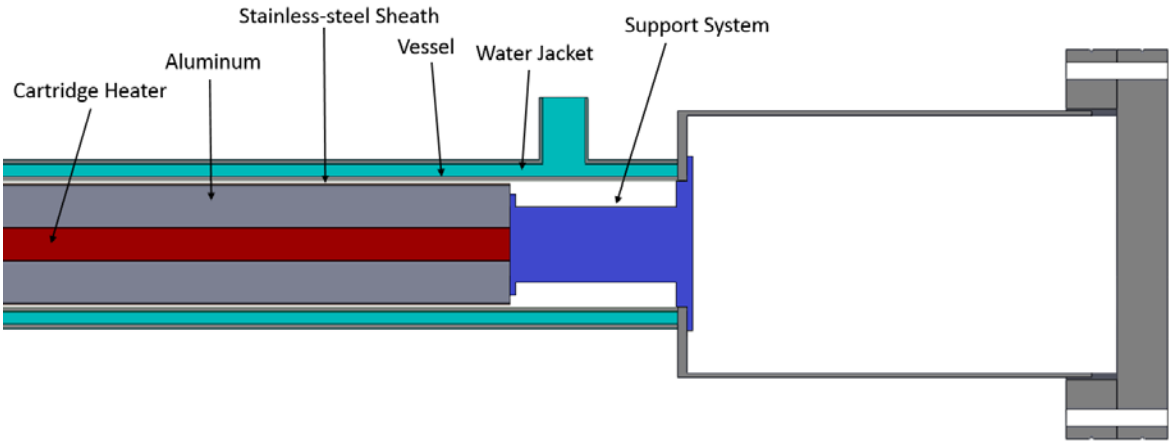

Figure 1: Schematic of one of the ends of experimental apparatus showing the different components.

where γ is the ratio of specific heats (γ= 5/3 for helium), Pr is the Prandtl number (Pr = 2/3 for helium), and α is the Thermal Accommodation Coefficient (TAC).

The TAC is defined as the fraction of energy a molecule exchanges with the wall that is interacting with it. Based on this definition, the TAC can be expressed using the incident T_i and reflected T_r temperatures as

$$\alpha = \frac{T_i - T_r}{T_i - T_w}. \tag{6}$$

The value of α varies from 0 to 1, where a value of 0 corresponds to specular reflection (the molecule does not transfer any of its energy to the wall, $T_r = T_i$), and a value of 1 corresponds to diffuse reflection (the molecule fully accommodates to the energy of the wall, $T_r = T_w$).

TAC values depend on several parameters, such as the wall material and its cleanliness, surface condition, and the nature of the gas [15]. Existing values for TAC for helium and stainless steel were compiled by Song and Yovannovich [16], and vary between 0.2 and 0.4 for temperatures between 700K and 300K, respectively.

Experiment Design

Figure 1 shows a schematic of one of the ends of the experimental apparatus used to measure heat transfer across rarefied helium gas. This experiment consists of two concentric cylinders spaced by a 2.0 mm helium-filled gap. The inner cylinder, shown in Fig. 2a, consists of a 12.7 mm diameter cartridge heater rod centered inside a thick aluminum cylinder, which is heat shrink fitted inside a 0.78 mm thick stainless steel cylinder to ensure optimum contact. The outer diameter of the inner cylinder is 43.5 mm. The outer cylinder consists of a pressure vessel of an inner diameter of 47.5 mm surrounded with a water jacket to control its temperature. The length of the inner cylinder is 1.118 m, and the length of the outer vessel cylinder is 1.422m. A support system attached to both ends of the inner cylinder, shown in Fig. 2b, is screwed to the outer cylinder to maintain concentricity between the two cylinders. The supports have small contact areas to prevent heat loss through conduction at the two ends of the inner cylinder and to ensure that most of the generated heat leaves through the annular gap between the cylinders.

To measure the temperature of the inner cylinder, twelve thermocouples were placed inside precision cut 1 mm deep channels on the outer surface of the aluminum cylinder (see Fig. 2a) at

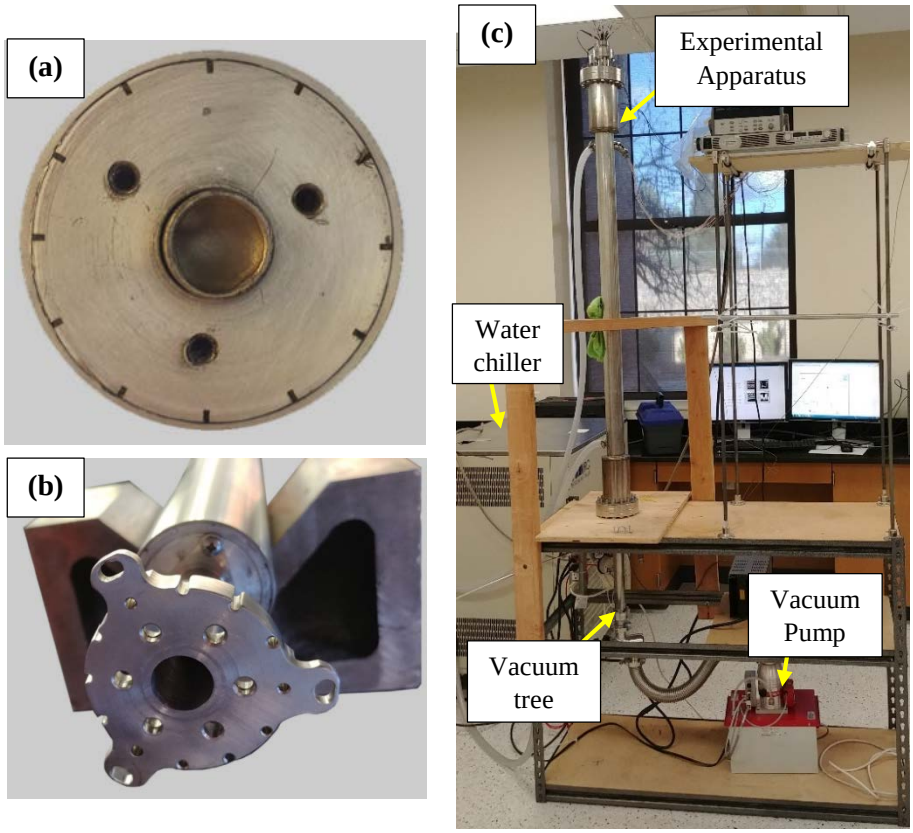

Figure 2: (a) A picture of one of the inner cylinder end showing thermocouple grooves, (b) a support attached to one end of the inner cylinder, and (c) assembled experiment standing upright

three different axial locations and secured with highly thermally conductive cement. Another twelve thermocouples are placed on the outer surface of the outer vessel cylinder at the same axial locations to measure its temperature as well.

Both ends of the pressure vessel cylinder are sealed using ultra-high vacuum ConFlat flanges. The bottom end of the experiment is attached to a vacuum tree that is connected to a pressurized helium tank through an open/close and leak valves and contains two low-pressure gauges and a vacuum pump. The other end has power and thermocouple feedthrough to connect the thermocouple and heater wires to the outside of the experiment. Figure 2c show a picture of the experimental apparatus fully assembled experiment and standing upright.

Determining TAC for Dry Helium

To determine the value of the TAC from the experimental results, an analytical expression that relates TAC to the temperature difference between the inner and outer cylinders is obtained in the slip regime.

Under the assumption that the temperature difference between the inner and outer walls is enough smaller than the average temperature ($\Delta T \ll T_{avg}$) and zero heat losses from the ends of the inner cylinder, and using the temperature jump boundary conditions at the gas-solid interfaces, the heat transfer by conduction between the inner and outer walls of the concentric cylinders experiment can be expressed as

$$Q_c = \Delta T \left(\frac{\lambda_i \zeta_{Ti}}{2\pi L r_i \kappa_i} + \frac{\ln \frac{r_o}{r_i}}{2\pi L \kappa} + \frac{\lambda_o \zeta_{To}}{2\pi L r_o \kappa_o} \right)^{-1}, \quad (7)$$

where Q_c is the heat portion transferred by conduction, L is the length of the inner cylinder, κ is the thermal conductivity of the gas, and r is the radius of the cylinders. The subscripts i and o are for inner and outer cylinders, respectively.

If we assume that the inner and outer cylinders have the same value of temperature jump coefficient and mean free path, and that the thermal conductivity in near constant between the two cylinders, then the equation for Q_c (7) can be simplified as

$$Q_c = 2\pi L \kappa \Delta T \left[\ln\left(\frac{r_o}{r_i}\right) + \lambda \zeta_T \left(\frac{1}{r_i} + \frac{1}{r_o}\right) \right]^{-1}. \quad (8)$$

Substituting the expression for temperature jump coefficient (5) and mean free path (2) into (8), the temperature difference between the inner and outer cylinders can be written as

$$\Delta T = \frac{Q_c}{2\pi L \kappa} \mu \frac{\sqrt{\pi}\gamma}{(\gamma+1)Pr} \left(\frac{2-\alpha}{\alpha} + 0.17\right) \left(\frac{1}{r_i} + \frac{1}{r_o}\right) \sqrt{\frac{2k_B}{m} T_o} \frac{1}{P} + \frac{Q_c}{2\pi L \kappa} \ln\left(\frac{r_o}{r_i}\right). \quad (9)$$

One can notice that equation (9) is linear with respect to the inverse of pressure. If we fit the experimental results of the temperature difference between the inner and outer cylinders as a function of the inverse of pressure with a first-order polynomial equation using the least square method as

$$\Delta T_{exp} = a \frac{1}{P} + b, \quad (10)$$

and compare the result to Eq. (9), the slope of the linear function, a, can be expressed as a function of the thermal accommodation coefficient as

$$a = \frac{Q_c}{2c_p L} \frac{\gamma}{\gamma+1} \left(\frac{2-\alpha}{\alpha} + 0.17\right) \left(\frac{1}{r_i} + \frac{1}{r_o}\right) \sqrt{\frac{2k_B}{\pi m} T_o}. \quad (11)$$

In Eq. (10), b is the intercept of the linear function. Equation (11) shows that the value of α depends only on the gas nature, the dimensions of the system, and heat flux, and do not depend on temperature-dependent parameters such as viscosity or thermal conductivity. Using this method, a single value of α can be determined for each heat generation rates.

Results and Discussion

Using the concentric cylinders apparatus, experiments were carried out for five total heat generation rates, Q_T, ranging from 95-476W and ten nominal pressures ranging from atmospheric (~10^5 Pa) to 110 Pa. The pressure range was chosen to cover both slip and continuum regimes. The temperature of the outer cylinder wall was maintained at 22°±1.0°C using the water jacket for all heat generation rates. Dry helium was used as the working fluid.

Figure 3 shows the experimental results of the temperature difference between the inner and outer cylinders as a function of pressure for all heat generation rates. The error bars shown in this

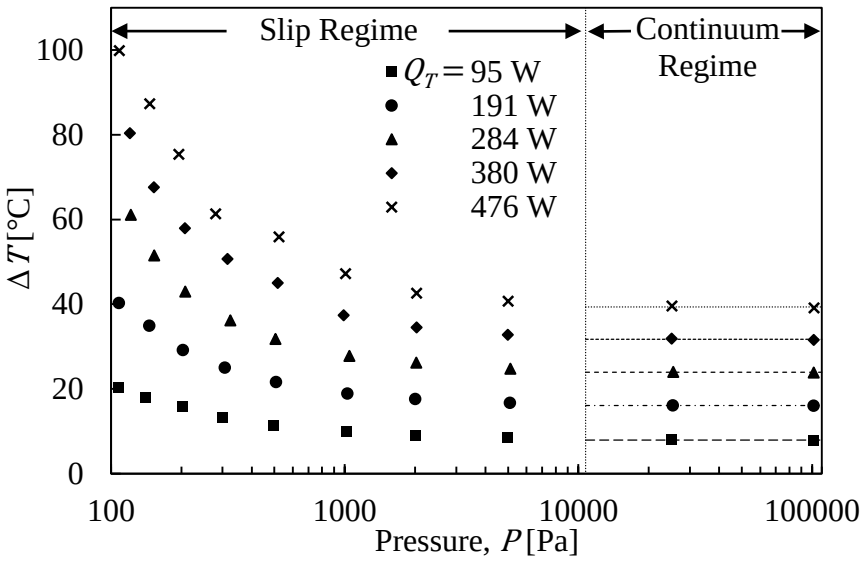

Figure 3: Measured temperature difference between the inner and outer cylinders as a function of pressure for all heat generation rates.

figure are calculated based on the thermocouples uncertainty of 1.1°C. Using the root sum square (RSS) method, the uncertainty on the temperature difference, $\Delta T = T_i - T_o$, is $w_{\Delta T}$ = 1.6°C. The vertical line shows the limit between the continuum and slip regime. This line correspond to the pressure of 10,736 Pa calculated using equations (1-3) for a Knudsen number of 10^{-3} and an outer wall temperature of 22°C. The horizontal lines are the average of the temperature difference for the three pressures in the continuum regime for each heat generation rate.

Figure 3 shows that the temperature difference is nearly constant in the continuum regime, which confirms the continuum assumption (no temperature jump at the gas-solid interfaces, $T_g = T_w$) in this regime. In the slip regime, one can notice in Fig. 3 that there a significant increase of the temperature difference as the pressure decreases. This increase is higher as the heat generation increases. The increase in temperature difference is of 12°C for Q_T = 95W and as high as 60°C for Q_T=476W. This increase is mainly due to the temperature jump that develops at the gas-solid interfaces and becomes significant in the slip regime. As shown by Eq. (4), the temperature jump increases as the pressure decreases or the heat generation rate increases.

Figure 4 shows the temperature difference between the cylinders as a function of the inverse of pressure for all heat generation rates. The profile of the temperature difference is linear with respect to the inverse of pressure, which confirms the assumptions made to obtain the analytical solution for heat transfer through an annular gap (Eq. 9). For each heat generation, the data points are fitted with a linear function according to equation (10), and the slopes (a) and intercepts (b) are obtained. The standard error of the estimate (E_{95}) at 95% confidence interval for the linear fit is calculated as

$$E_{95} = 2\sqrt{\frac{\sum\left(a\frac{1}{P} + b - \Delta T\right)^2}{N-2}}, \qquad (12)$$

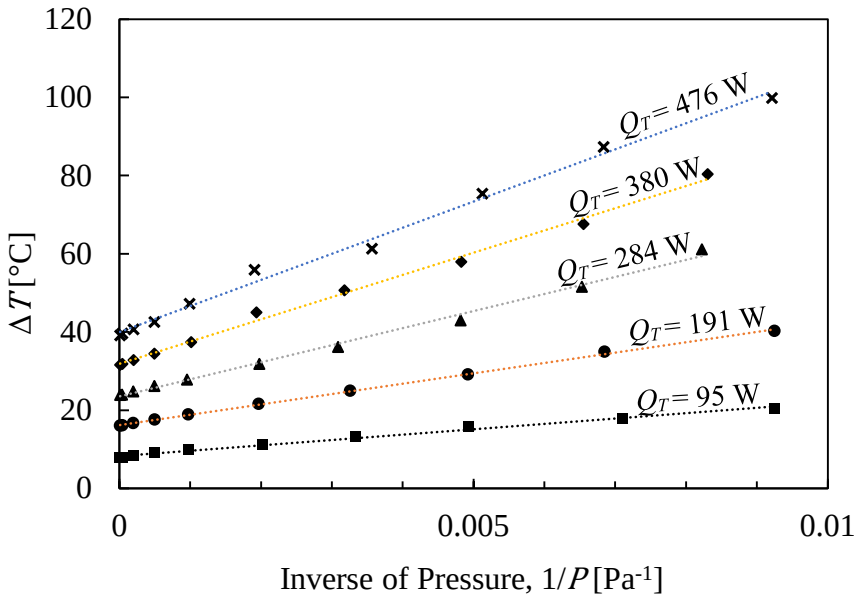

Figure 4: Measured temperature difference between the inner and outer cylinders as a function of the inverse of pressure for all heat generation rates.

where N is the number of measurements. The value of E_{95} is estimated for each heat generation rate and is listed in Table 1. This table shows that the value of E_{95} increases as a function of the heat generation rate, except for Q_T = 191W, where its value slightly decreased. The value of E_{95} is smaller than the uncertainty on the temperature difference, $w_{\Delta T}$ = 1.6°C, for Q_T = 95 and 191 W, and larger for the other heat generation rates. It should be reminded here that equation (9) was obtained under the assumption that the temperature difference between the cylinders is smaller than the average temperature. As the heat generation increases, this assumption starts to breakdown, which explains the large values of E_{95} obtained at high heat generation rates. At Q_T = 476 W and P = 109 Pa, ΔT is about 29% of the average temperature.

To use Eq. 11 to calculate the thermal accommodation coefficient from the value of the slope (a) for each heat generation, the amount of heat transferred by conduction, Q_c, has to be calculated. To do this, an average value of the radiative heat transfer between the cylinders for all pressures is calculated and subtracted from the total heat generation rate as

$$Q_C = Q_T - Q_R, \tag{13}$$

where Q_R is the heat transferred by radiation. The emissivity for the inner and outer cylinders were measured to be 0.152 and 0.149, respectively.

Table 1: Standard error of the estimate for a 95% confidence interval for the linear fit, and values of the thermal accommodation coefficient and uncertainty for all heat generation rates

Q_T [W]	E_{95} [°C] (95%)	T_{avg} [°C]	α	w_α
95	0.9	33	0.36	0.03
191	0.6	46	0.37	0.02
284	1.9	58	0.35	0.02
380	2.4	69	0.35	0.02
476	3.6	82	0.37	0.03

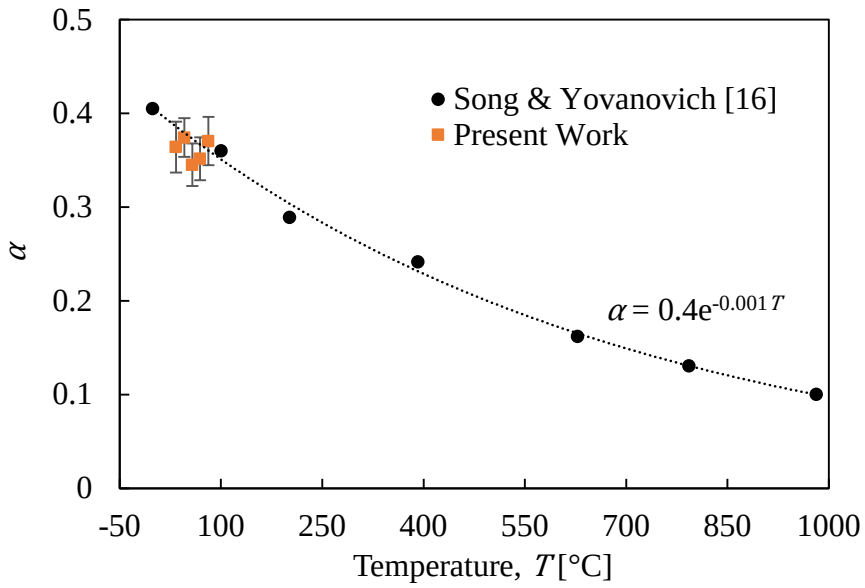

Figure 5: Comparison of the value of the thermal accommodation coefficient, α, for helium on stainless steel surface obtained from literature [16] and present work

Table 1 shows the value of the thermal accommodation coefficient, α, obtained for each heat generation rate using Eq. (11). This value is between 0.35 and 0.37 for all heat generation rates. For each value of α, the corresponding temperature is calculated as the average of inner cylinder temperatures, T_{avg}, over the whole range of pressure for each heat generation rate. These values are also given in Table 1.

Figure 5 shows the value of the thermal accommodation coefficient, α, as a function of the temperature for helium gas on stainless steel surface compiled by Song and Yovanovich, 1987 [16]. The values of α exhibit an exponential decay as a function of temperature. The values of α obtained from the concentric cylinder experiment (Table 1) are also included in Fig. 4 and are represented by square symbols. This figure shows that there is a good agreement between the experimental values of α obtained in this work and the values found in the literature.

Conclusion and Future Work

The low-pressure conditions during the vacuum drying process of UNF casks can have a significant effect on the temperature of the fuel cladding. As the pressure of helium in the cask decreases, the temperature of the cladding may considerably increase due to the temperature-jump that develops at the gas-solid interfaces. The thermal accommodation coefficient is an important parameter that affects the temperature jump. In this work, an experimental apparatus was designed and built to measure heat transfer across rarefied helium and to calculate the thermal accommodation coefficient for helium on stainless steel surface. Values of α were obtained between 0.35 and 0.37 for temperatures between 33°C and 82°C. These values are in good agreement with data reported in the literature.

For future work, the concentric cylinders experiment will be used to measure the thermal accommodation coefficient for moist helium and water vapor. To the best of our knowledge, no data of thermal accommodation coefficient is available in the literature for water vapor.

Acknowledgments

This work was supported by the U.S. Department of Energy Office of Nuclear Energy University Program under award number DE-NE0008713 and U.S. Nuclear Regulatory Commission under award number NRC-HQ-13-G-38-0027.

References

[1] W. Large, "Review of drying methods for spent nuclear fuel," Savannah River Site (US), 1999.

[2] U.S. Nuclear Regulatory Commission, "Standard review plan for spent fuel dry storage systems at a general license facility," *NUREG-1536 Rev*, vol. 1, 2010.

[3] ASTM, "ASTM C1553-16, Standard Guide for Drying Behavior of Spent Nuclear Fuel, ASTM International, West Conshohocken, PA, 2016, www.astm.org.

[4] S. Schaaf and P. Chambré, "Flow of Rarefied Gases" Princeton University Press, Princeton, NJ, 1961.

[5] U.S. Government Printing Office, "10, Code of Federal Regulations, Part 72, "Energy: Licensing Requirements for the Independent Storage of Spent Nuclear Fuel and High-Level Radioactive Waste, and Reactor-Related Greater than Class C Waste," Office of Federal Register National Archives and Records Administration, Washington, DC, 2008.

[6] U.S. Nuclear Regalotory Commision, "Cladding Considerations for the Transportation and Storage of Spent Fuel," Interim Staff Guidance Report for the Spent Fuel Project Office of the U.S. NRC, ISG-11 R3, 2003.

[7] R.S. Daum, S. Majumdar, and M.C. Billone, "Experimental and Analytical Investigation of the Mechanical Behavior of High-Burnup Zircaloy-4 Fuel Cladding," *J. ASTM Intern*., 5(5), 2008.

[8] M. Billone, T. Burtseva, and R. Einziger, "Ductile-to-brittle transition temperature for high-burnup cladding alloys exposed to simulated drying-storage conditions," *Journal of nuclear materials*, vol. 433, no. 1-3, pp. 431-448, 2013.

[9] R. S. Daum, S. Majumdar, Y. Liu, and M. C. Billone, "Radial-hydride embrittlement of high-burnup Zircaloy-4 fuel cladding," *Journal of nuclear science and technology*, vol. 43, no. 9, pp. 1054-1067, 2006.

[10] M. Billone, T. Burtseva, and Y. Liu, "Baseline properties and DBTT of high-burnup PWR cladding alloys," in *Proc. PATRAM*, 2013, pp. 18-23.

[11] G. Bird, "Definition of mean free path for real gases," *Physics of Fluids*, vol. 26, no. 11, pp. 3222-3223, 1983.

[12] G. Bird, "Molecular Gas Dynamics and the Direct Simulation of Gas Flows (Oxford Engineering Science Series)," *Clarendon*, 1994.

[13] F. Sharipov, "Data on the velocity slip and temperature jump coefficients," in *5th International Conference on Thermal and Mechanical Simulation and Experiments in Microelectronics and Microsystems, 2004. EuroSimE 2004.* Proceedings of the 2004 IEEE, pp. 243-249.

[14] J. T. Lin and D. Willis, "Kinetic theory analysis of temperature jump in a polyatomic gas," *Physics of Fluids*, vol. 15, no. 1, pp. 31-38, 1972.

[15] F. O. Goodman, "Thermal accommodation coefficients," *Journal of Physical Chemistry*, vol. 84, no. 12, pp. 1431-1445, 1980.

[16] S. Song and M. Yovanovich, "Correlation of thermal accommodation coefficient for engineering surfaces," *ASME HTD*, vol. 69, pp. 107-116, 1987.